Deep-Sea Research II 98 (2013) 7–23

Contents lists available at ScienceDirect

Deep-Sea Research II

journal homepage: www.elsevier.com/locate/dsr2

Condor seamount (Azores, NE Atlantic): A morpho-tectonic interpretation

Fernando Tempera [a,*], Ana Hipólito [b], José Madeira [c], Sara Vieira [a], Aldino S. Campos [d], Neil C. Mitchell [e]

[a] Centre of IMAR of the University of the Azores, DOP & LARSyS, Rua Prof. Dr. Frederico Machado, no. 4, PT-9901-862 Horta, Açores, Portugal
[b] Centro de Vulcanologia e Avaliação de Riscos Geológicos, Universidade dos Açores, Complexo Científico, 3° Piso – Ala Sul, Rua da Mãe de Deus, 9500-321 Ponta Delgada, Açores, Portugal
[c] Departamento de Geologia da Faculdade de Ciências & Instituto Dom Luiz (Laboratório Associado), Universidade de Lisboa, C6, Campo Grande, 1749-016 Lisboa, Portugal
[d] Portuguese Task Group for the Extension of the Continental Shelf (EMEPC), Rua Costa Pinto 165, 2770-047 Paço de Arcos, Portugal
[e] School of Earth, Atmospheric and Planetary Sciences, University of Manchester, Williamson Building, Oxford Road, Manchester M13 9PL, UK

ARTICLE INFO

Available online 21 September 2013

Keywords:
Condor
Seamounts
Multibeam
Volcanism
Tectonics
Erosion features
38°24′N–38°38′N
29°16′W–28°51′W

ABSTRACT

High-resolution datasets collected by multibeam and acoustic backscatter surveys were used to produce fine-scale seafloor nature and morpho-tectonic interpretations of the Condor seamount. Condor constitutes an elongated volcanic ridge that extends for 39 km and rises more than 1800 m from the surrounding seafloor. Constructive morphologies include (i) linear eruptive centres, (ii) volcanic cones with or without summit depressions, (iii) lava flows and (iv) hummocky sectors. Eruptive type is interpreted to vary with depth. On the deeper seamount extremities, the predominance of highly acoustically backscattering volcanic cones and hummocky terrain is interpreted to result from effusive eruptions not yet covered by sediment deposits. In contrast, the smoother relief of the central seamount flanks is interpreted as draping and infilling of the underlying effusive relief by (i) primary volcaniclastic deposits produced by explosive eruptions on the shallowest parts of the ridge, together with (ii) secondary volcanigenic sediments resulting from truncation of the seamount top by swell erosion and (iii) sediments resulting from biogenic production.

A set of WNW–ESE to NW–SE trending volcano-tectonic structures are shown to control most of the fissural volcanism that formed the ridge. A network of NNW–SSE trending faults is identified on the seafloor around Condor but they show little relation with the distribution of volcanic edifices or with post-emplacement dismantling of the seamount. These fault sets are related to the transtensional regime acting on the Azorean segment of the Eurasia–Nubia plate boundary.

Erosional features include (i) palaeo wave-cut platforms on the seamount summit, (ii) landslide scars produced by lateral collapses of the NE and SW-facing flanks, (iii) gullies and turbidity current channels and (iv) mass-wasting deposits. Iceberg drag and bump marks are also identified on the seamount upper flanks, representing the first reference to such features in the Azores and an additional low latitude record.

Given the lack of major erosional and tectonic dismantling, Condor is suggested to be a relatively young seamount. A revised factoring of eustatic, erosional and isostatic processes does not exclude that the summit may have been eroded as late as the Last Glacial Maximum.

1. Introduction

Seamounts are some of the most ubiquitous landforms on Earth and their time-averaged generation may represent 10–20% of the global cumulative magmatic extrusive budget (Wessel, 2007). They occur at ridge-transform fault intersections, overlapping spreading centres, in intraplate regions and hotspots (*e.g.*, Iyer et al., 2012). The most recent desktop extraction of seamounts from a global bathymetric grid at 30″ resolution (Yesson et al., 2011) identified 33,452 seamounts (*i.e.*, height ≥ 1000 m) plus 138,412 smaller elevations (200 m ≤ height < 1000 m).

With the development and widespread use of high-resolution acoustic systems such as multibeam echo-sounders and sidescan sonars over the last few decades, detailed morphological analyses of seamounts were made possible. Seamounts were revealed to

* Corresponding author. Tel.: +351 292 200400; fax: +351 292 200411.
E-mail addresses: tempera@uac.pt (F. Tempera), ana.rc.hipolito@azores.gov.pt (A. Hipólito), jmadeira@fc.ul.pt (J. Madeira), amscampos@emepc-portugal.org (A.S. Campos), neil.mitchell@manchester.ac.uk (N.C. Mitchell).

0967-0645/$ - see front matter © 2013 Elsevier Ltd. All rights reserved.
http://dx.doi.org/10.1016/j.dsr2.2013.09.016

range from flat-topped conical elevations with and without summit craters or collapse pits to dome-shaped structures and linear ridges. Important insight on how tectonic and volcanic processes control the constructional and erosional processes responsible for shaping seamounts was provided by Fornari et al. (1987), McPhie (1995), Smoot (1995), Mitchell (2001), Johnson et al. (2008) and Passaro et al. (2010).

With only a small extent of the Azores geology being accessible on the subaerial parts of the islands, knowledge of the seafloor is critical to understand the geodynamic processes acting around the Azores oceanic plateau.

Linear volcanic ridges (LVRs) have been shown to be the most common geomorphological feature in the Azores region, Northeast Atlantic (Lourenço et al., 1998). LVRs are composite volcanic constructions built by basaltic fissural volcanism which in the Azores is favoured by the transtensional tectonic environment.

Condor is a large LVR located in the vicinity of Azorean island of Faial. It has been the target of an intense scientific programme for the last 4 years, aiming to improve our understanding of seamount structure and functioning from the sea surface down to the seafloor (see Giacomello et al., this issue).

Although having been surveyed with the Towed Ocean Bottom Instrument (TOBI) during the AZZORRE'99 cruise (Ligi et al., 1999), the earliest published information on the geomorphology of Condor can only be found in Lourenço et al. (2008). In their analysis of the main volcano-tectonic structures found around Faial, Condor was identified as a LVR and a brief illustrated description of its back-scatter patterns was provided. More recently, Tempera et al. (2012) presented an overview of the seamount's geological and biological landscape based on new high resolution multibeam mapping of the seafloor and benthic surveys.

Using the multibeam compilation of Tempera et al. (2012) along with new groundtruth information, the current paper details a geomorphological interpretation of Condor, providing (i) a morpho-structural map of the area and (ii) a seafloor facies map. Tectonic structures, volcanic and erosional forms and seabed nature are mapped in fine scale supported by groundtruthing provided by remotely operated vehicles (ROVs) and drop-down cameras.

1.1. Geological background of the area

The Azores archipelago lies about the boundaries between the North America (NA), Eurasia (Eu) and Nubia (Nu) plates at the Azores Triple Junction (ATJ; Fig. 1). The Azores portion of the Eu–Nu plate boundary is expressed as a wide dextral transtensional zone (*e.g.* Lourenço et al., 1998; Madeira and Ribeiro, 1990; Madeira and Brum da Silveira, 2003), where hyper-slow oblique expansion occurs (Vogt and Jung, 2004), accommodating the differential

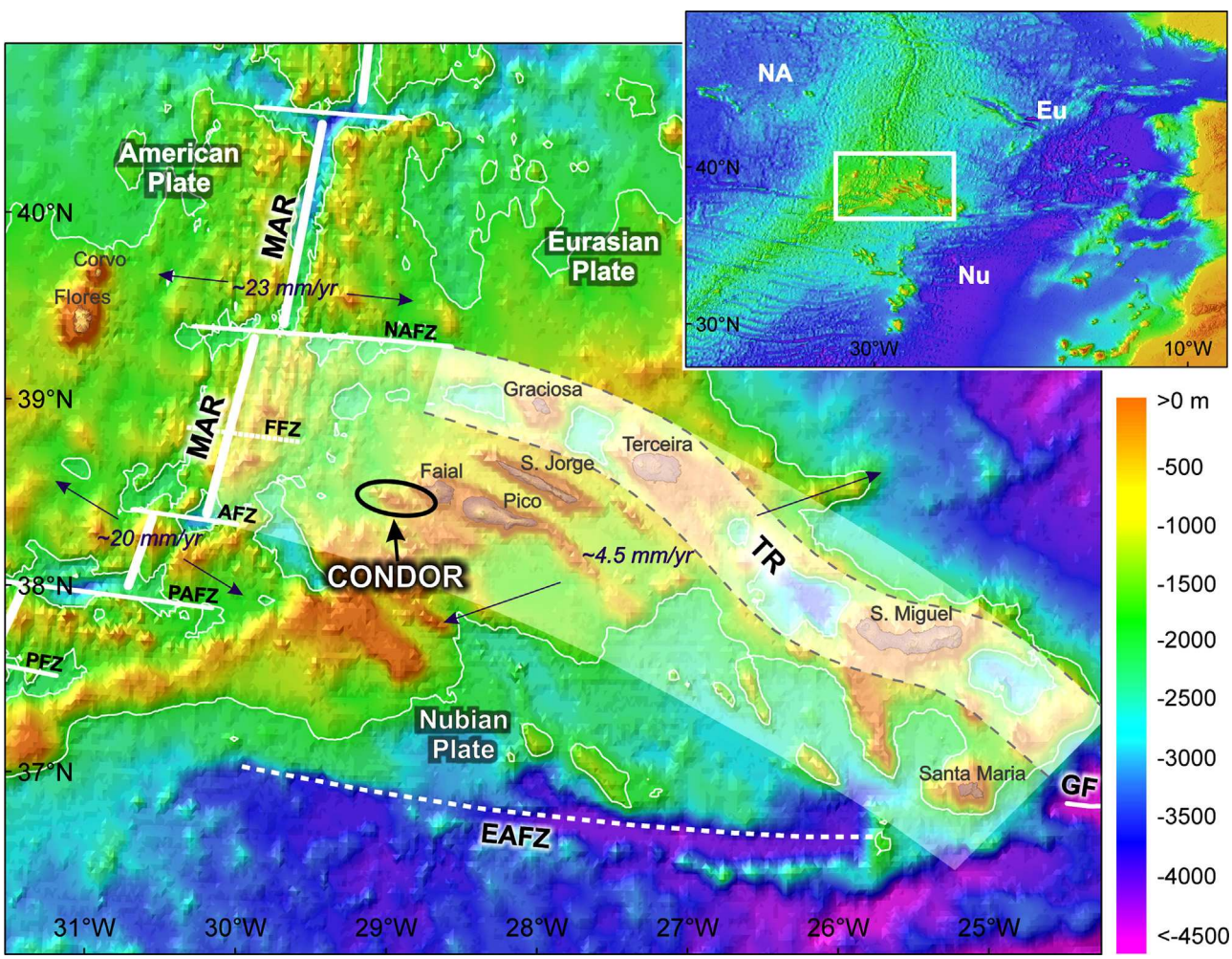

Fig. 1. Location of Condor seamount in the general frame of the Azores. White lines define approximately the morphological expression of each structure; white shaded area represents the sheared western segment of the Eurasia–Nubia plate boundary; white shaded area limited by a dotted grey line represents its main structure, the Terceira Rift (TR). Tectonic structures: MAR–Mid-Atlantic Ridge; EAFZ–East Azores Fracture Zone; NAFZ–North Azores Fracture Zone; GF–Gloria Fault; FFZ – Faial Fracture Zone; AFZ–Açor Fracture Zone; PAFZ–Princesa Alice Fracture Zone; PFZ–Pico Fracture Zone. Azores bathymetry sourced from Lourenço et al. (1998) and GEBCO 08. Datum: WGS 1984.

motion between the Eu and Nu plates (*e.g.* DeMets et al., 1994, 2010; Fernandes et al., 2003; Mendes et al., 2013). Progressive northward relocation of the plate boundary from the abandoned East Azores Fracture Zone (Luis and Miranda, 2008), created a triangular area of elevated and anomalously thick ocean crust (*e.g.* Dias et al., 2007; Hirn et al., 1980; Luís et al., 1998) named the Azores Plateau (Needham and Francheteau, 1974). Based on topographical, seismic, geochemical and gravity data some authors suggested that the ATJ is interacting with a hotspot (*e.g.* Cannat et al., 1999; Gente et al., 2003; Madureira et al., 2005; Schilling, 1975; Silveira et al., 2006).

The complexity of this area is commonly reflected in the volcanic and seismic activity that affects the islands and the surrounding offshore areas. The northern limit of the shear zone is relatively well constrained to the area immediately to the northeast of the Graciosa – S. Miguel alignment – the so-called Terceira Rift (TR; *e.g.* Machado, 1959; Searle, 1980; Fig. 1). From roughly west of Graciosa and Faial islands towards the Mid-Atlantic Ridge (MAR), the Eu–Nu plate boundary loses its topographic identity (*e.g.* Lourenço et al., 1998). Surveys by Luís et al. (2007) revealed this area to be largely lacking volcanic edifices but dominated by a complex fault pattern

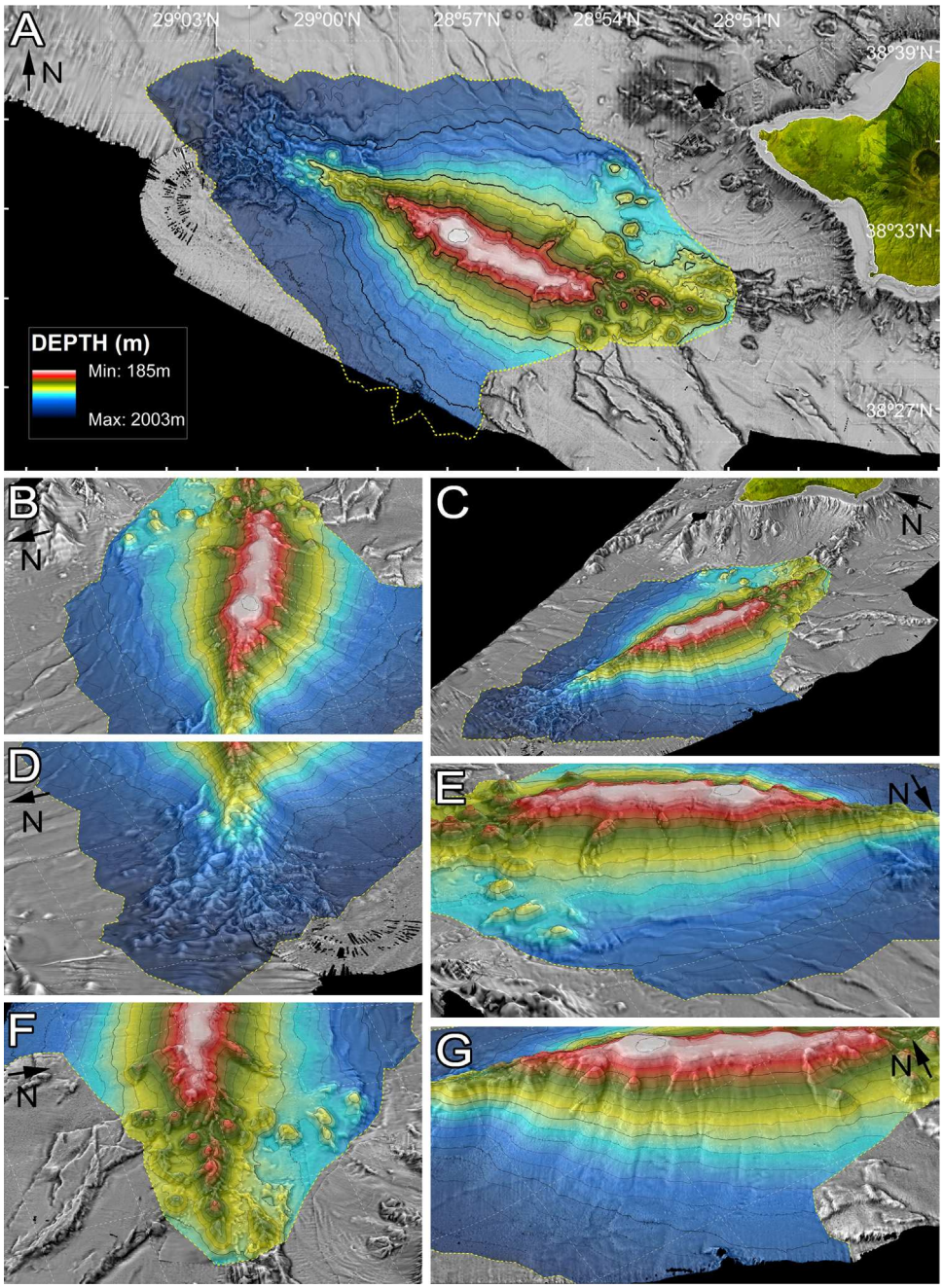

Fig. 2. Plan view and 3D perspectives of different sectors of the Condor seamount. (A) Plan view with delimited seamount extent (yellow dashed line and enclosed coloured area); (B) view along the ridge approximately from WNW; (C) view of the seamount off southwestern Faial; (D) view of the western seamount extremity exhibiting anastomosed extrusions; (E) view of the northern flank of the ridge approximately from NNE exhibiting a few outcrops and extensive smooth area blanketed by sediments. A faulted ocean floor area is visible at its base; (F) view of the eastern seamount extremity; (G) view of the southern flank of the ridge approximately from SSW. (For interpretation of the references to color in this figure legend, the reader is referred to the web version of this article).

that is still under investigation in order to clarify the location of the present-day ATJ.

Condor seamount is located 100 km from the MAR, on the southern margin of the westernmost stretch of the Eu–Nu plate boundary (Fig. 1). The seamount overlies ocean floor formed between anomalies 4 and 5, which corresponds to a period between 7.01 and 10.10 Ma (Luís et al., 1994). Morphologically, Condor constitutes an elongated volcanic ridge that extends for 39 km and rises more than 1800 m from the surrounding seafloor (Fig. 2). The WNW–ESE trend of the seamount's major axis is parallel to other volcanic ridges found in the area, including the Faial-Pico and the S. Jorge volcanic ridges, and the structural trend of the TR between Terceira Island and the West Graciosa basin.

2. Material and methods

2.1. Data acquisition

Multibeam bathymetry and backscatter data were collated from various acoustic surveys performed over the seamount and its vicinity. The main surveys were conducted in 2008 and 2010 by NRP *Almirante*

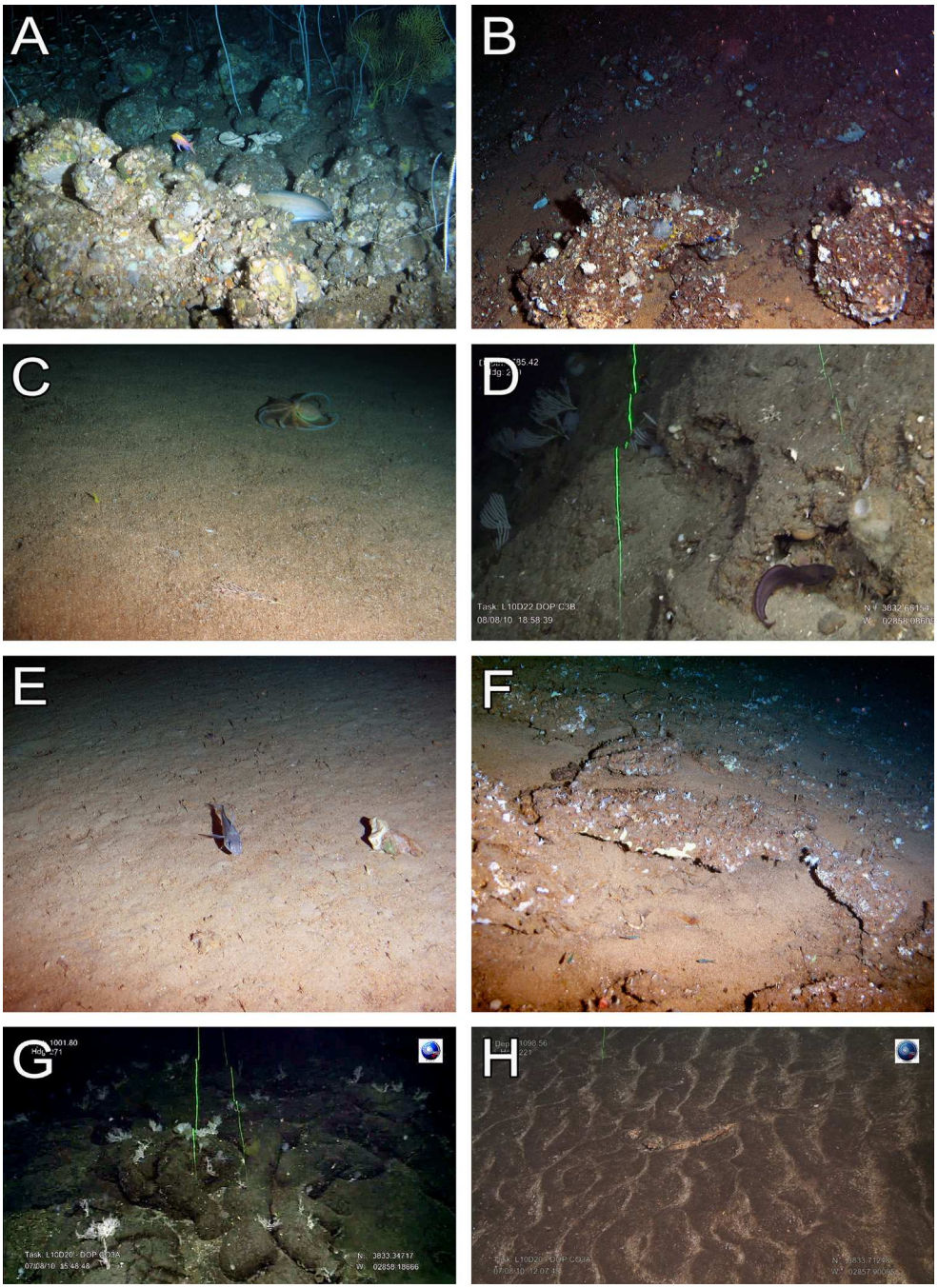

Fig. 3. A selection of seafloor types observed on the Condor seamount. (A) Rounded beach boulders on the planated summit. (B) Angular boulders on the shallowest summit. (C) Sandy substrate on the summit. (D) Consolidated carbonates on the northern flank. (E) Muddy substrate on the northern flank. (F) Sedimentary seafloor with surficial plates on the southern flank. (G) Pillow lavas on the northern flank. (H) Volcanic sand at the current-swept base of the northern flank. Image credits: (A,B,C,E,F) © Greenpeace/Gavin Newman; (D,G,H) DOP-UAz/EMEPC. The location of each image on the seamount is shown in Fig. 8A.

Gago Coutinho, using a 12-kHz Kongsberg-Simrad EM120 swath bathymetry sonar. The data were acquired using the Seafloor Information System (SIS) package and processed using CARIS HIPS & SIPS, where layout, attitude and sound velocity corrections were introduced and spurious data removed. An additional dataset covering the NW sector of the seamount was sourced from the 2006 STRIPAREA cruise where swath bathymetry was acquired using a 30-kHz Simrad EM300 sonar. The post-processed data from the different surveys were extracted as regular grids with a cell size of 20 m and subsequently merged in an ArcGIS environment. The bathymetric grid used in the scope of this work covered a total area of 1112 km^2, including the seamount and the neighbouring slope of Faial Island.

Multibeam backscatter mosaics were produced in CARIS HIPS & SIPS v. 7.0 (in the case of the 2008 and 2010 datasets) and in MB-System v. 5.1.2 (in the case of the 2006 dataset). Processing included both geometrical correction (bottom tracking, removal of altitude and slant range correction) and elementary radiometric compensation (beam angle). Final mosaics had a resolution of 10 m. A backscatter mosaic produced in PRISM from a dataset collected in 1999 using the deeply towed sidescan sonar TOBI was used as complementary information (data courtesy of Marco Ligi, ISMAR-CNR, Italy). Physical sampling of the seafloor was restricted to the sediment cores and grab material analysed in Zeppilli et al. (this issue). Apart from this, abundant seafloor optical imagery was sourced from surveys that visited a total of 25 different locations on the seamount summit and flanks, covering a total transect length of 34 km (Fig. 3). Multiple optical platforms were used that included (i) a customized 2000 m-rated drop-down camera (2006), (ii) the 6000 m-rated ROV *Luso* (2008, 2010) and (iii) the 300 m-rated ROV *SP* (2009 – 2011). The footage collated was annotated using the COVER software ©IFREMER, including geo-referenced information on substrate nature that were used during backscatter interpretation.

2.2. Morpho-tectonic analysis

The bathymetric and backscatter maps were visually inspected in ArcGIS environment to identify the features and geomorphological structures described below in this section.

2.2.1. Seamount extent

The elevated area corresponding to the seamount has been delineated using (i) the farthest convex bathymetric contours radiating from the main ridge and (ii) intersection lines with other geomorphic features (island slope, other reliefs and surrounding plains).

2.2.2. Seafloor nature

Backscatter mosaics were integrated in the ArcGIS project (*e.g.*, Fig. 4C) and used as a basis for a human-assisted interpretation of seabed nature (consolidated *vs.* unconsolidated) at a scale of 1:20,000 (Fig. 5A). Interpretation of tonal and textural backscatter properties followed Blondel and Murton (1997). In situations where backscatter exhibited insufficient quality, the demarcation of the rocky areas was assisted by (i) an examination of the geomorphological context, (ii) seafloor type information derived from groundtruthing surveys and (iii) bathymetric texture in the form of high-resolution slope and sun-illuminated relief maps. Using this complementary information was particularly relevant to improve the substrate delineation in areas where acoustic backscatter was only provided by the TOBI backscatter mosaic. Because of towfish-ship location uncertainties, this dataset was poorly registered with respect to the multibeam bathymetry at the fine scale used.

2.2.3. Submarine geomorphologic features

The constructive volcanic forms identified on Condor are those considered in Table 1. They include all geomorphologic features with positive elevation built by accumulation of volcanic products namely pyroclastic fall deposits, lava flows and pyroclastic density currents (PDCs).

Erosional forms comprise the features detailed in Table 2 and formed by destructive processes such as erosion (including abrasion) and mass wasting.

The tectonic features identified in the study area include the structures described in Table 3.

3. Results

The new compilation of multibeam bathymetry and visualization resolves the surface geomorphology of the Condor seamount in enhanced detail, permitting updating morphometric characteristics presented in Tempera et al. (2012) (Figs. 2, 4A and 6). It is now established that the seamount ranges over 1818-m in elevation, with its shallowest point at 185 m depth and its deepest point at 2003 m. Its revised outline forms an elongated lozenge in plan view, with a major semi-axis of 39 km and a minor semi-axis of 23 km (yellow dashed line in Fig. 2). This polygon has a plan area of 493.4 km^2 and a surface area of 512.2 km^2 (at 20 m resolution), resulting in a *surface to area ratio* of 1.038.

3.1. Substrate nature

The seamount extent polygon and a classification of its surface in consolidated substrate and non-consolidated sediment is shown in Fig. 5A. The interpretation extends slightly beyond the limits of topography since some backscatter data (namely the mosaic derived from the TOBI survey) ranged beyond the available multibeam bathymetry compilation. Overall, 68% (corresponding to 335.1 km^2) is covered by sedimentary or volcaniclastic material with the remaining 32% (*i.e.*, 158.2 km^2) corresponding to consolidated surfaces. A small selection of images illustrating some of the seafloor diversity found is shown in Fig. 3.

The distribution of substrates of distinct nature with depth is presented in Fig. 5B, which shows that consolidated substrates are more common than unconsolidated sediments down to 800 m depth. An analysis with the geomorphology indicates that high backscatter is produced by apparently fresh volcanic edifices (cones and ridges) making up the eastern and western extremities of the Condor Complex. Shallower than 800 m depth the consolidated substrate comprises mainly the planated high backscatter surfaces dominating the seamount summit (where they represent ~80% by area), the central ridge and a few flank outcrops. The high backscatter exhibited by the summit suggests a hard substrate composition that strongly contrasts with the flanks and is shown by seafloor imagery to correspond to large rocky outcrops, rounded boulders and gravels, attesting its wave-induced abrasion origin (Tempera et al., 2012).

The low backscatter apron that characterizes the flanks of the central seamount sector is interestingly concentric with the 400–500 m isobaths. This observation suggests that most of the explosive eruptions producing significant amounts of fine volcaniclastic particles occurred above this depth.

3.2. Geomorphological interpretation

The morpho-tectonic interpretation of the Condor seamount is shown in Fig. 7.

3.2.1. Constructional volcanic forms

The volcanic edifices found in the study area are dominated by the three main types described in Table 1: (i) *submarine volcanic*

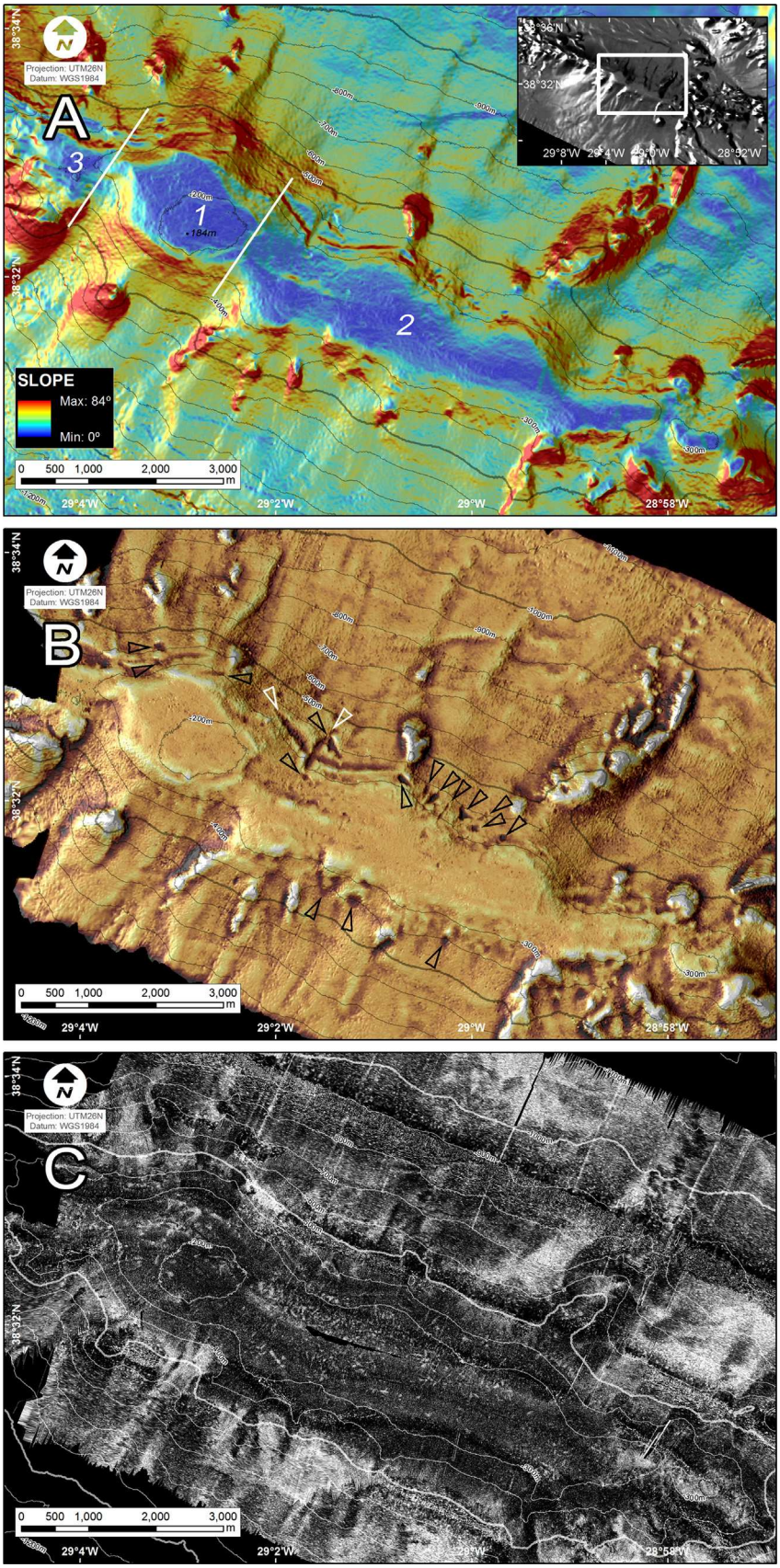

Fig. 4. Condor seamount summit plan views. (A) Slope map (B) Ridge-and-trough enhanced relief with arrows signalling a suite of long indentations and bump marks along the upper flank interpreted as iceberg ploughmarks. (C) Backscatter mosaic with dark tones representing high reflectivity areas.

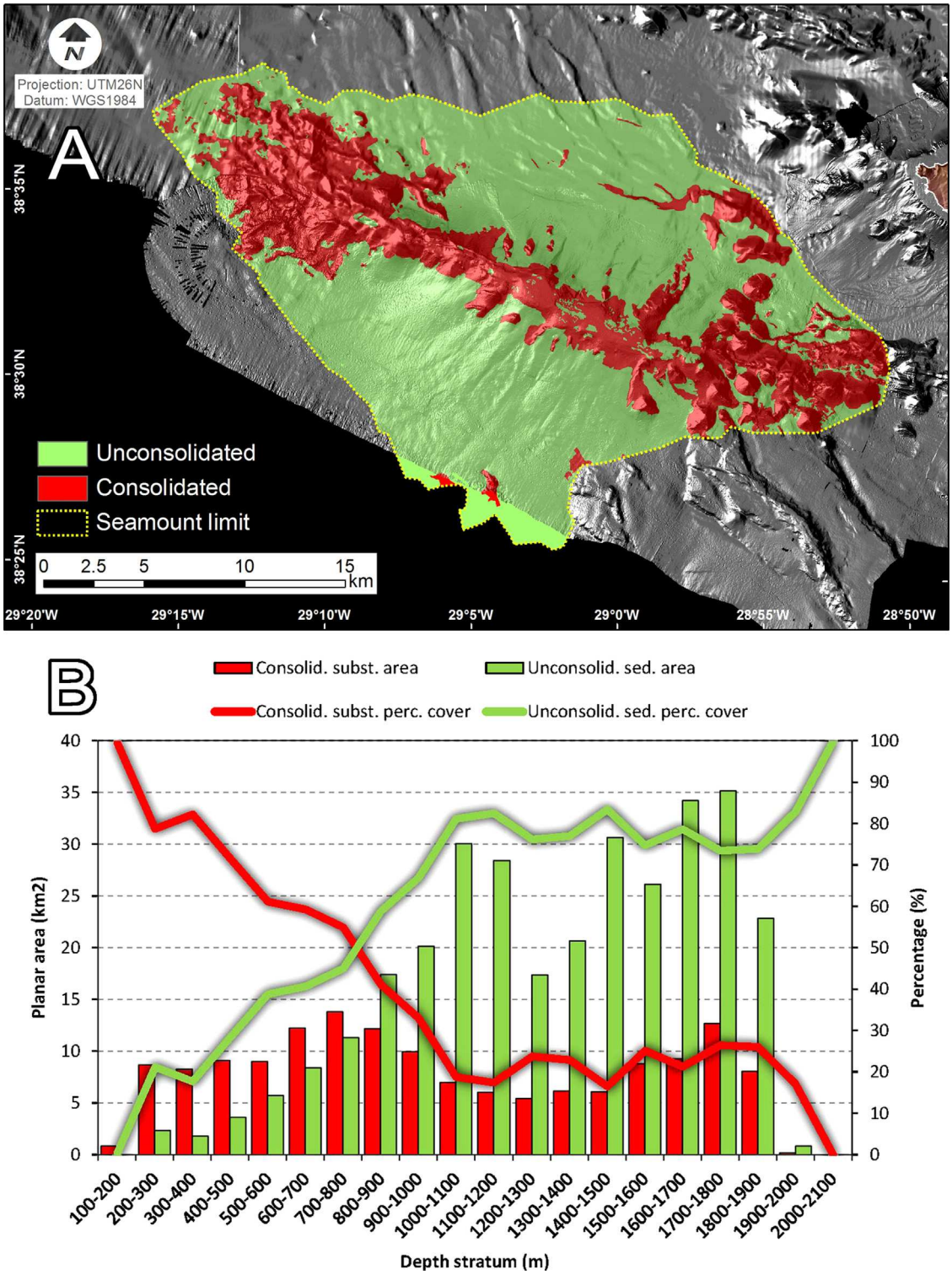

Fig. 5. (A) Distribution of consolidated *vs.* non-consolidated substrates on the Condor seamount based on backscatter interpretation supported by seafloor video imagery; (B) substrate nature distribution per 100 m depth stratum.

cones; (ii) *linear eruptive centres* and (iii) *unclassified submarine volcanic forms* (Figs. 5A and 6).

The eastern sector is dominated by an extremely irregular terrain dotted by a population of sub-circular cones with heights between 50 and 300 m (Table 4). A distinct subset of volcanic edifices is located on the WNW extremity of the ridge which is characterized by irregular bases, low height-to-diameter ratio and apparently well-developed craters or collapse pits.

A geometric analysis of average height (Hco) and basal width (Wco) was made for a total of 23 volcanic cones using the method of Favalli et al. (2009). Individual measurements are listed in Table 4 and were used to build the Hco *vs.* Wco scatterplot presented in Fig. 8. All cones analysed have Hco/Wco ratios lower than the 30° gradient expected if the flanks were formed of volcanic talus at the angle of repose (Mitchell et al., 2000, 2012). A number of cones (blue numbers in Fig. 8A and blue triangles in

Table 1
Description of the constructive forms recognized on the Condor seamount.

Cone-shaped eruptive centres (or submarine volcanic cones)	Positive geomorphologic features exhibiting a sub-circular conical morphology with basal diameter up to 1630 m and height up to 350 m. They occur in isolation, aligned parallel to the axial direction of Condor, or in clusters. Although they most commonly exhibit smooth un-eroded slopes, a few cones seem to present small landslide scars on their flanks. With a few exceptions, they generally lack a summit crater or collapse pit
Craters or collapse pits	Bowl-shaped depressions at the summit of volcanic cones. Delineation of these structures follows the top edge of the depression. Some of these forms were quite incipient at the grid resolution used. Other more or less prominent edges delimiting indistinct forms were classified as 'undeterminate rims' (see next)
Undeterminate rim	Edge structures that could not be categorically classified as a crater or collapse pit or as a landslide scar
Linear eruptive centres	Elongated morphologies that often occur in clusters forming linear chains parallel to each other. Their alignment is clearly parallel to the regional tectonic trends and to the trend of Condor itself. Some of them result from eruptions along linear vents, whereas others result from overlapping of aligned cones
Unclassified volcanic forms	This category represents all positive geomorphic features of atypical shape that could not be unequivocally classified. They probably result from features (perhaps eruptive edifices) in an advanced state of erosion
Wave-eroded unclassified volcanic forms	Unclassified volcanic forms whose summit is slightly flattened at the same depth as the paleo wave-cut platform
Lava flows	Relatively smooth surfaces extending downslope from cones or linear eruptive centres. Some of them form small lava plateaus with steep fronts
Hummocky surfaces	Irregular and undulated topography comprising a set of small, non-linear, generally chaotic and rounded rises and lows with multidirectional slopes. Most of these surfaces are usually related with lava flows or mass movements

Table 2
Description of the erosional forms recognized on the Condor seamount.

Paleo wave-cut platform	Flat area that cuts across the summit of the rising seamount flanks. It forms a narrow platform which is interpreted as a product of wave abrasion. The platform is divided into three main levels, differing in their degree of development
Erosional gullies/channels	Relatively straight or V-shaped shallow incisions formed in moderate to steep slopes. These are the most common erosional features observed on the seamount flanks. They are formed by the interaction of slope failures and the resulting fluid or sediment flows moving downslope
Fan/Mass-wasting deposits	Convex-up, irregular surfaces located downslope of small slide scars located on volcanic cones or ridges. Some undulated surfaces associated with erosional gullies on the seamount flanks were interpreted as downslope mass transport deposits
Landslide scars	Typical arcuate headwall scars of semi-ellipsoidal to amphitheatre-like morphology. These features cut across the paleo wave-cut platform and, more rarely, the flanks of volcanic cones. Each scar can be the result of a single event but potentially multiple events may have left complex superimposed multiple failure scars. Where the scar did not show a typical geometry of instability features (*e.g.* soft morphology), it was classified as an 'undeterminate rim'
Toreva blocks	Large coherent features (megablocks) located downslope of inferred scars related to large landslides. They occur within volcaniclastic fan deposits and are interpreted as large sections of the edifice that slid downslope without disaggregation
Volcaniclastic apron	Seamount slopes draped by smooth deposits of marine and volcanogenic sediments formed *in-situ*, re-sedimented or transferred downslope by subaqueous gravity flows. Its outer edges were defined based on the distinct break in slope and convex-up contours. These deposits generally exhibit low acoustic backscatter
Volcanic outcrops	All irregular reliefs with typically high backscatter and a configuration suggesting constructive hard relief structures. Several of them emerge from the sedimentary/volcaniclastic blanket that covers the central sectors of the ridge flank

Table 3
Description of the tectonic forms recognized on the Condor seamount.

Fault scarps	Linear steps on the seafloor surface corresponding to the most explicit tectonic structures that cut the seafloor surrounding the seamount. The symbols delineating fault scarps are placed along the fault trace due the small scale of the map used
Inferred faults	Other morphological lineaments likely produced by tectonics
Volcanic alignments	Linear eruptive centres and aligned volcanic cones interpreted as further indicators of underlying tectonics controlling volcanic extrusion

Fig. 8B) show a high Hco/Wco ratio and relatively homogeneous morphometric characteristics, a possible indicator of youth. In contrast, a smaller set of cones exhibit lower than average ratios (Fig. 8B). These more flattened profiles may result from erosion (*e.g.* cone 19; Fig. 8A) or tectonic disruption (*e.g.* cone 17; Fig. 8A).

A correlation between depth and edifice type is particularly noticeable on the eastern extremity of Condor: elongated edifices apparently concentrate on the deeper areas whilst conical edifices prevail on shallower areas closer to the coast of Faial island.

Convex circular to lobate shapes were found in the areas between some cones and ridges and, in some cases, partially overlapping older edifices (Figs. 5A and 6). The original interpretation of this hummocky morphology as fissure-erupted pillow flows (Smith and Cann, 1992) was recently demonstrated by ROV observations presented in Searle et al. (2010). The absence of nearby slide scars argues against them being debris flow/avalanche deposits.

Only four lava flows have been mapped. One has a considerable size and probably represents a compound flow forming a thick lava terrace. We speculate that this is a result of a succession of lava flows from a single prolonged eruptive episode (Fig. 7). Further identification and mapping of lava flows was hindered by data resolution which is insufficient for resolving surficial features of flows such as compression ridges, fronts or digitiform lobes.

3.2.2. Erosional features

The planated summit in the central part of the seamount likely corresponds to surfaces truncated by swell abrasion and eventually some degree of subaerial erosion (Figs. 2 and 3A). Three major subhorizontal surfaces can be recognized at different average depths. The shallowest planated surface comprises the western seamount summit (1 in Fig. 4A), exhibiting depths averaging 203 m (S.D.: 11) and an average slope of 2.6°. An elongated ridge with a flattened,

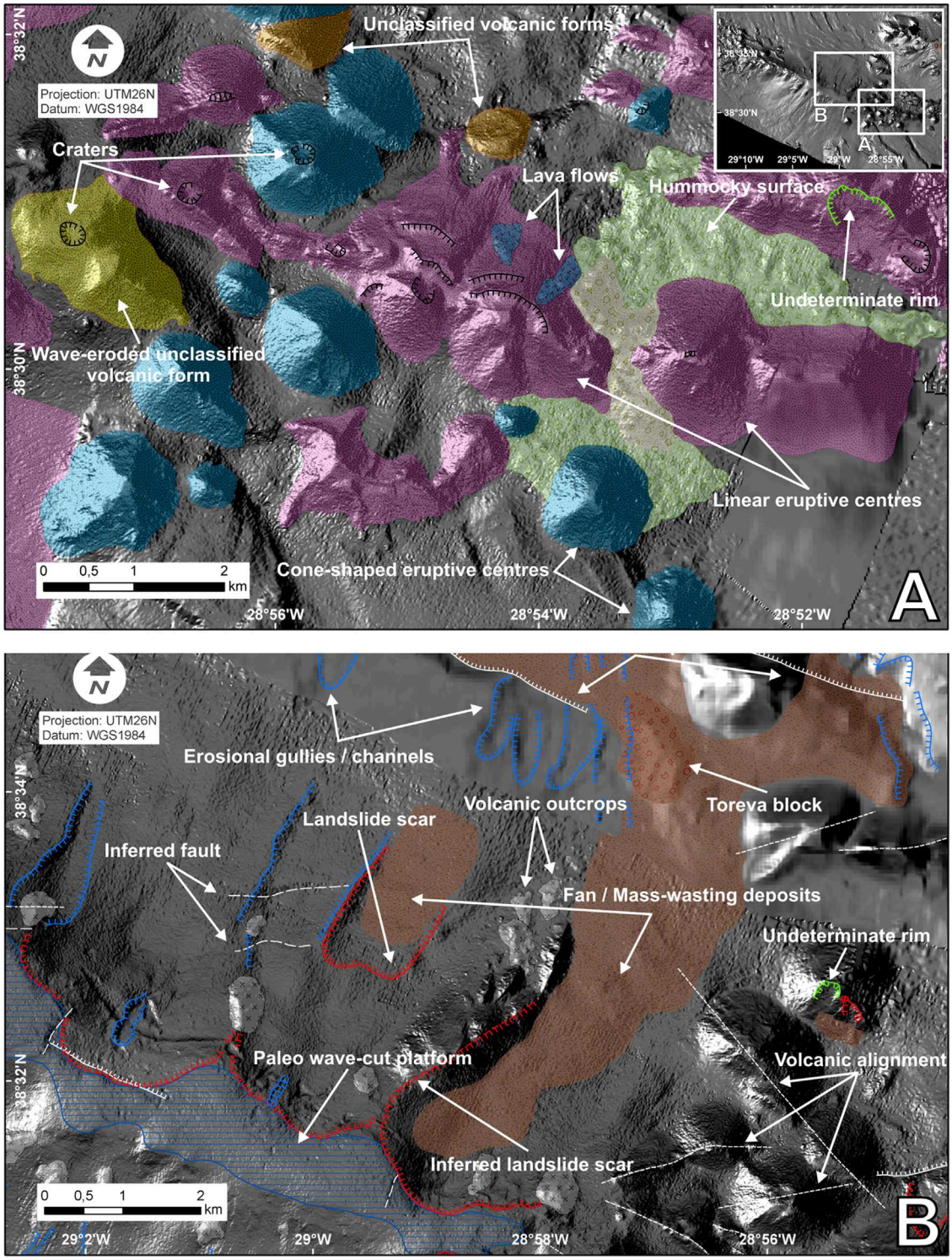

Fig. 6. Highlights of delineated geomorphologic features. (A) Constructive volcanic forms and (B) destructive volcanic forms.

though slightly convex, profile (2 in Fig. 4A) is present to the east of the former sector, exhibiting an average depth of 237 m (S.D.: 14) and an average slope of 3.6°. A smaller additional subhorizontal surface (3 in Fig. 4A) is identifiable to the west of sector 1 at depths averaging 303 m (S.D.: 3) with a mean slope of 3.3°.

The most disseminated erosional features on sloping ground are mass wasting scars that range in width between a few hundred metres and a few kilometres. They indent (i) fault scarps, (ii) the flanks of small monogenetic edifices, (iii) the margins of the top abrasion platform and (iv) the seamount slopes. Landslide deposits are typically found downslope of the headwall scars that, on the seamount slopes, exhibit a higher backscatter than the surrounding undisturbed volcaniclastic apron. The larger deposits are generally fan shaped and composed of smooth disintegrated material exhibiting an undulated morphology. Only one of these deposits located to the NE of the seamount includes a probable toreva block, implying that sections of the seamount flank slid without major disaggregation.

It is uncertain whether wide embayments where no mass wasting headwalls were identified actually represent interfluves

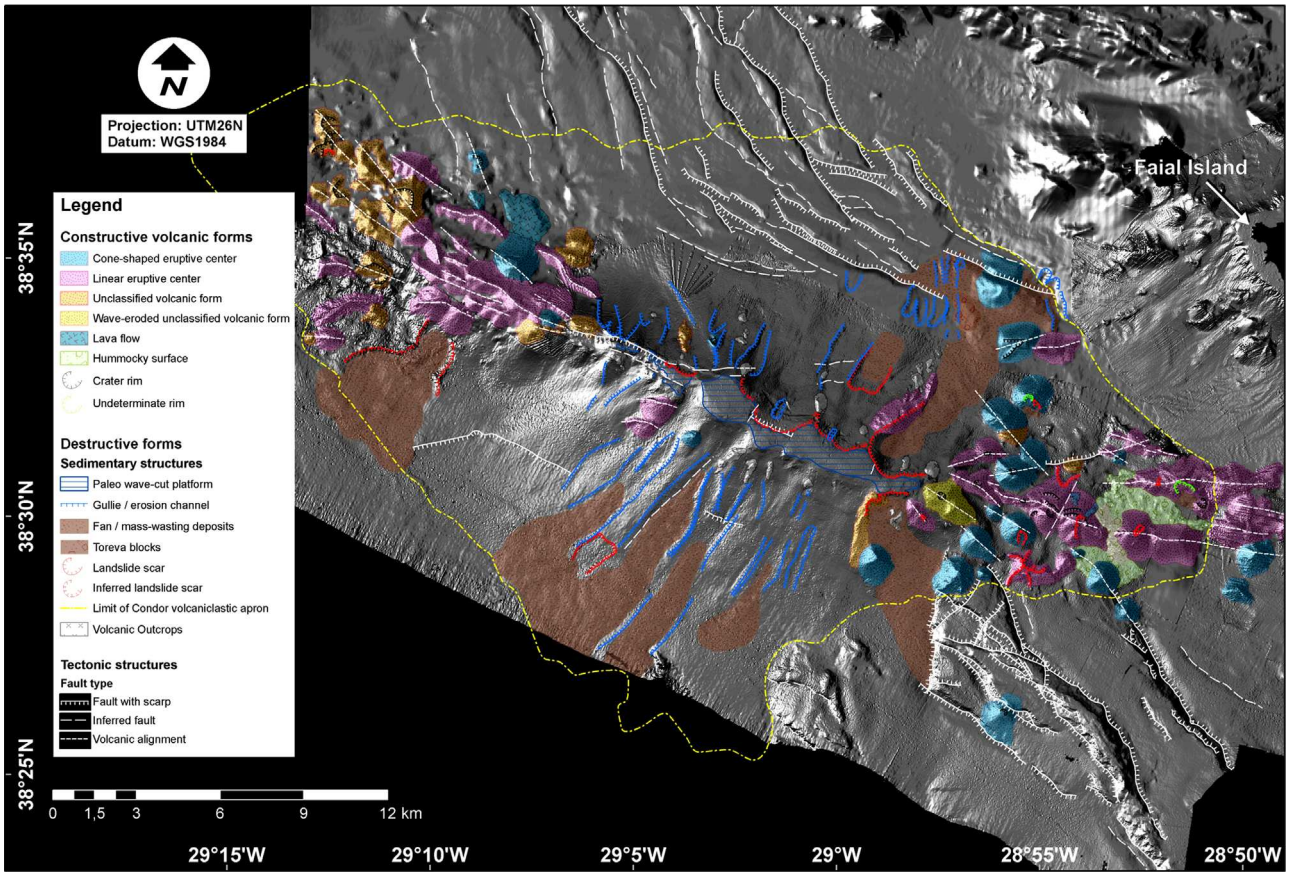

Fig. 7. Morpho-structural interpretation of Condor geomorphology, highlighting constructional and destructive morphological features.

Table 4
Main morphometric parameters of the cone-shaped eruptive centres mapped on Condor area, using the calculation method of Favalli et al. (2009) for the average of heights (Hco) and basal widths (Wco).

Cone ID	Hco (m)	Wco (m)	Aspect ratio (Hco/Wco)	Summit depth (m)
1	287	1348.3	0.213	−557
2	253	1407.4	0.180	−534
3	119	528.7	0.225	−688
4	283	1201.1	0.235	−453
5	124	574.1	0.216	−551
6	309	1242.5	0.249	−416
7	96	423.4	0.226	−715
8	283	1189.4	0.238	−654
9	154	879.5	0.175	−835
10	176	968.0	0.182	−898
11	212	1053.7	0.201	−654
12	297	1325.7	0.224	−419
13	293	1334.4	0.219	−703
14	102	493.8	0.207	−908
15	131	639.7	0.205	−408
16	85	491.9	0.174	−562
17	156	1539.2	0.101	−773
18	211	1543.0	0.136	−889
19	48	743.1	0.064	−1750
20	341	1629.9	0.209	−1020
21	113	656.4	0.172	−668
22	267	1365.9	0.195	−817
23	250	1295.9	0.193	−754

between volcanic massifs that coalesced throughout seamount build-up and were smoothed by the volcaniclastic blanket (Fig. 7). Incipient erosion gullies/channels occur in some of these embayments which act as conduits for gravitational transport of sediment down the flanks (Figs. 2, 6B and 7). A few semi-circular embayments found on conical edifices at the seamount extremities could not be established as slide scars or laterally-collapsed volcanic craters.

At finer scales it is worth mentioning the presence of one 2.2 km-long arcuate incision at 358–378 m depth along the northern flank of the seamount which is intersected at approximately its mid length by another linear incision oriented roughly perpendicular to it (white arrows in Fig. 4B). Other smaller depressions are present further along the northern margin of the seamount, roughly in the same 300–400 m depth range (black arrows in Fig. 4B). A few smoother indentations are visible on the southern flank at the same depth range. Morphological traits (Fig. 4A and B) include (i) raised berms of generally 1 m, (ii) indentation depth of up to 11 m (iii) widths between 72 and 250 m, (iv) elongated shapes along the dip of sloped morphologies. These characteristics suggest drag or bump marks produced against steep slopes, which are consistent with the marks produced by iceberg keels (*e.g.*, Dowdeswell et al., 2010; Hill et al., 2008).

3.2.3. Tectonic pattern

The tectonic structures affecting the Condor area define two main fault systems (Fig. 9):

(1) A set of structures trending WNW–ESE to NW–SE that is mainly associated with the eruptive fissures that controlled the build-up of Condor. Two families of normal faults, dipping in opposite senses, can be identified. Features belonging to this set include (i) fault scarps attaining *ca.* 100 m height and showing few or no volcanic extrusions and (ii) alignments

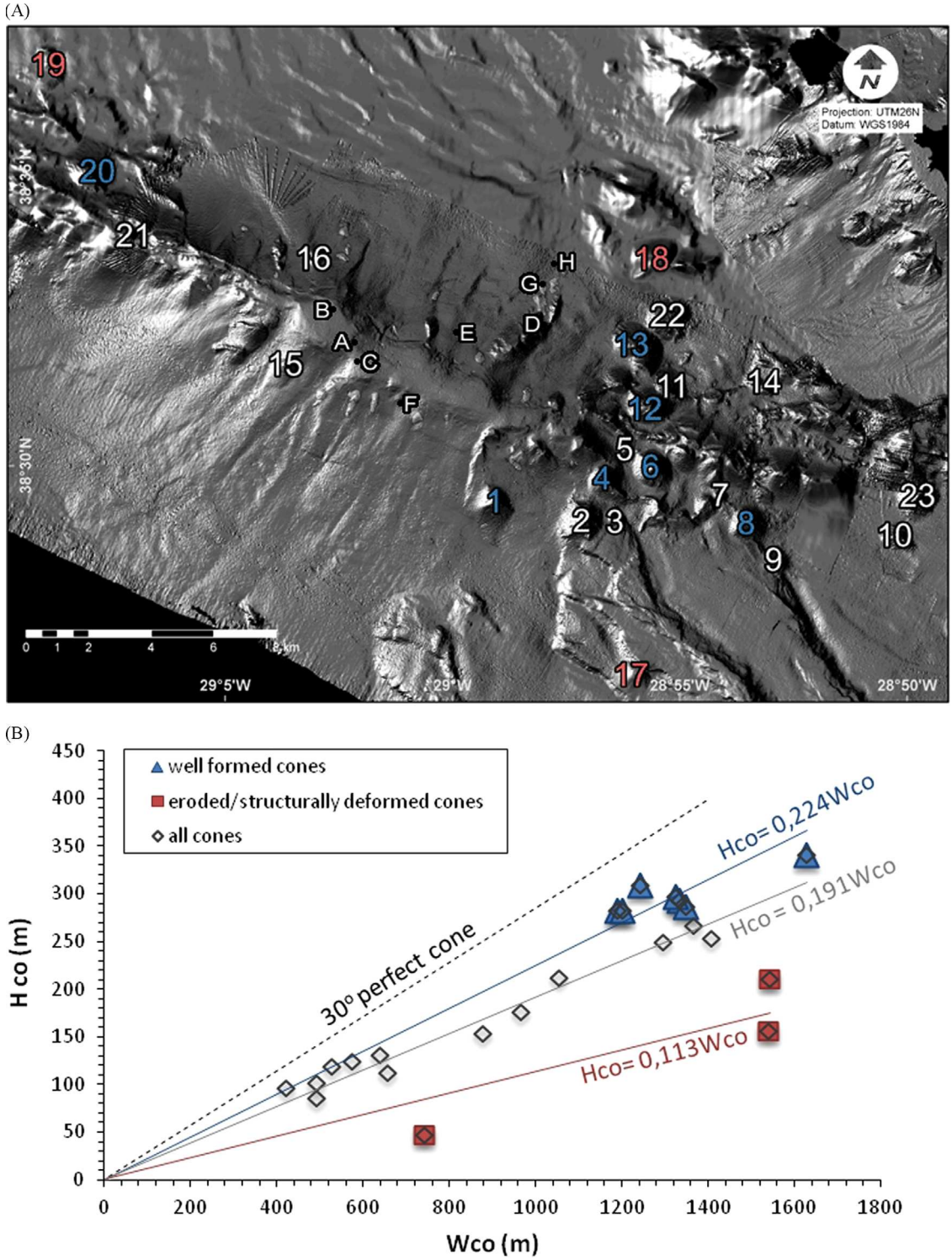

Fig. 8. Morphometric analysis of volcanic cones identified in Condor area. (A) Location of the cones (with reference numbers) and of the seafloor images from Fig. 3 (with reference letters). (B) Height (Hco) *versus* width (Wco) scatterplot with a dashed reference correlation line representing the trend expected for a perfect cone with 30° flank. (For interpretation of the references to colour in this figure, the reader is referred to the web version of this article.)

of volcanic edifices, namely the ridge itself or smaller cone alignments. Close to the eastern tip of the seamount these structures merge with E–W trending fractures.

(2) A second set of normal faults, also presenting two opposite dips, trend NNW–SSE. This network of faults shapes the ocean floor NW and SE of the seamount producing a horst-graben morphology that exhibits well-developed scarps attaining heights up to 200 m. Apart from a structure on the SE sector that seemingly controlled the emplacement of a few volcanic cones along this direction, this system generally lacks interaction with extrusive processes, similarly to what is known from emerged areas of the archipelago (*e.g.*, Madeira and Brum da Silveira, 2003).

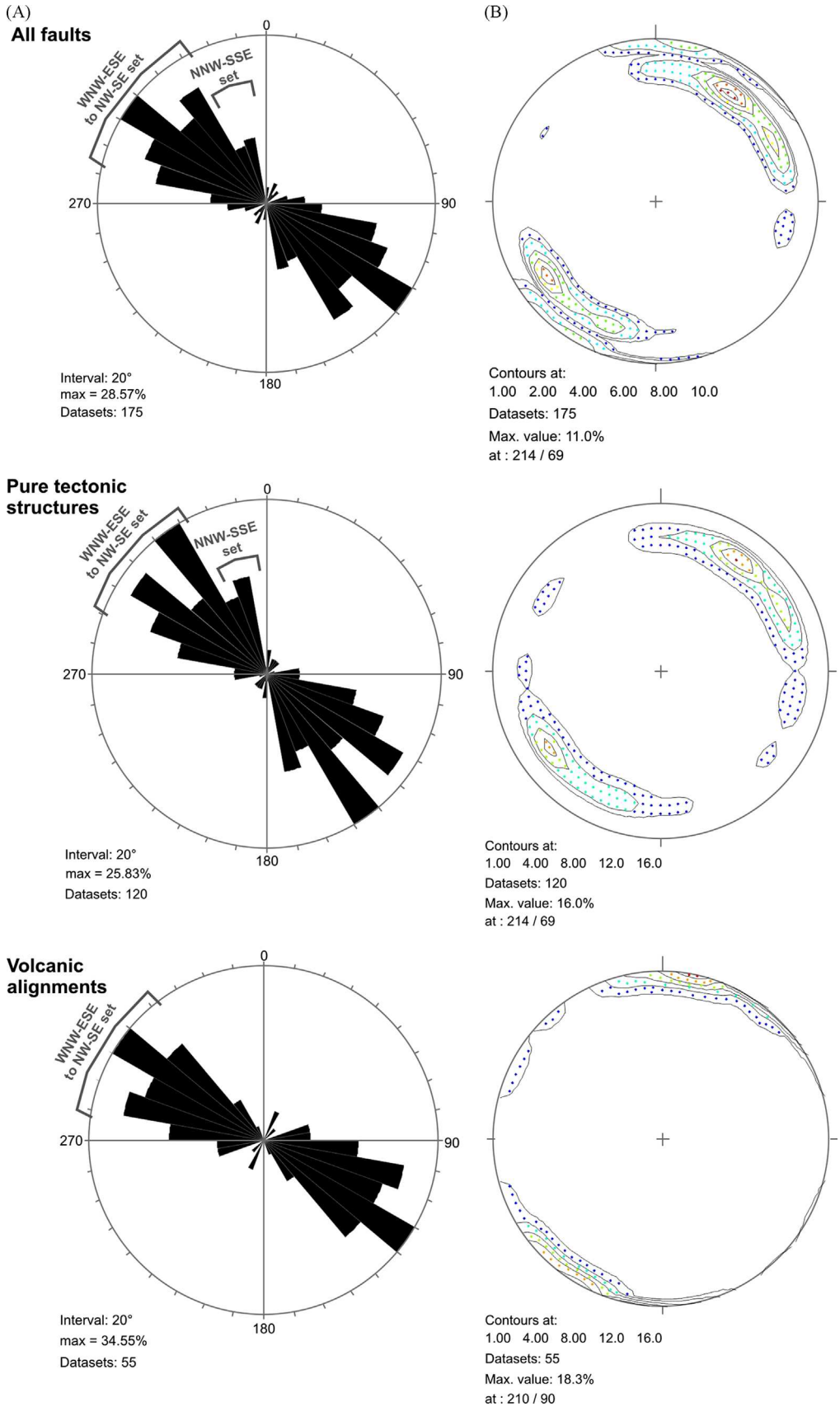

Fig. 9. Geometry of tectonic structures, considering *all faults*, *pure tectonic structures* and *volcanic alignments*. (A) Circular histograms of unweighted frequencies; (B) contour plots of fault pole density (lower hemisphere; Schmidt net). TectonicsFP software® (Ortner et al., 2002).

A small number of structures trend NNE–SSW to N–S and ENE–WSW to NE-SW, but they do not influence the morphology of the seamount. On the SE sector of the surveyed area, these are represented by fault scarps and volcanic lineaments.

4. Discussion

4.1. Tectonic setting

The WNW–ESE to NW–SE trending structures control most volcanism on Condor. In contrast, the well-developed NNW–SSE-oriented tectonic structures that cross the older ocean floor surrounding the seamount show little relation with the volcanic structure of the submarine ridge, without any post-emplacement tectonic deformation, or with dismantling processes affecting the edifice. The presence of the same two sets of faults observed elsewhere in the central and eastern Azores Islands (Carmo et al., in press; Hipólito et al., in press; Madeira, 1986, 1998; Madeira and Brum da Silveira, 2003; Madeira et al., in press) suggests that the area is under the same right-lateral transtensional tectonic regime that dominates this area of the Eu–Nu plate boundary (*e.g.* Lourenço et al., 1998; Madeira, 1998). Hence, the Condor seamount is a volcanic ridge, built off-MAR on top of 7.01–10.10 Ma old seafloor (Luís et al., 1994), along a WNW–ESE fracture that presents an *en échelon* arrangement relatively to the Faial-Pico ridge. The exact location of this volcanic structure may also be favoured by the intersection with the conjugated fault system, as observed in most major central volcanoes in the archipelago.

The WNW–ESE tectonic structures, which control most of the tectono-magmatic processes in the Azores spreading centre, merge to with E–W trending structures east of Condor ridge. The set of E–W trending structures is aligned with the south coast of the island of Faial that presents similar trend (Fig. 10). These structures can be interpreted as representing former transform faults locally cutting the old deep ocean crust onto which the Azores Plateau was built. The orientation of these fractures favours its reactivation by the present stress field and may be used to link segments of *en échelon* WNW–ESE structures, as seen in several onshore areas (Madeira, 1998). This fact highlights the importance of E–W fractures in the tectonic pattern of the Azores as already proposed by Gaspar (1996) and Madeira (1998).

4.2. Magmatism and ridge morphology

The elongated morphology of Condor and lineaments of monogenetic volcanic edifices found on its extremities typify a linear volcanic ridge (*e.g.* Höskuldsson et al., 2007; Searle et al., 1998, 2010). Instead of being produced by a central volcano developing from a magma reservoir, this type of linear volcanic edifices forms from a system of fissures opened by seafloor rifting and offering a preferential pathway for magma to ascend along the seamount axis.

In slow-spreading rate settings, the ridge edification is commonly controlled by along-axis changes in melt supply (*e.g.* Pierce and Sinha, 2008). The NW tip of the seamount shows a global dendritic shape, which should be the resulting morphology of both linear-fissure pillow lava eruptions along diverging fault splays and flank lateral collapses. Contrastingly, the SE extremity is characterized by the presence of several isolated cones and ridges aligned in a dominant direction. Hence, it is assumed that in an early stage of Condor's formation high volumes of magma likely ascended through an extensive network of dykes that efficiently extruded lavas through linear fissure-fed eruptions, preferentially oriented along what would become the main seamount

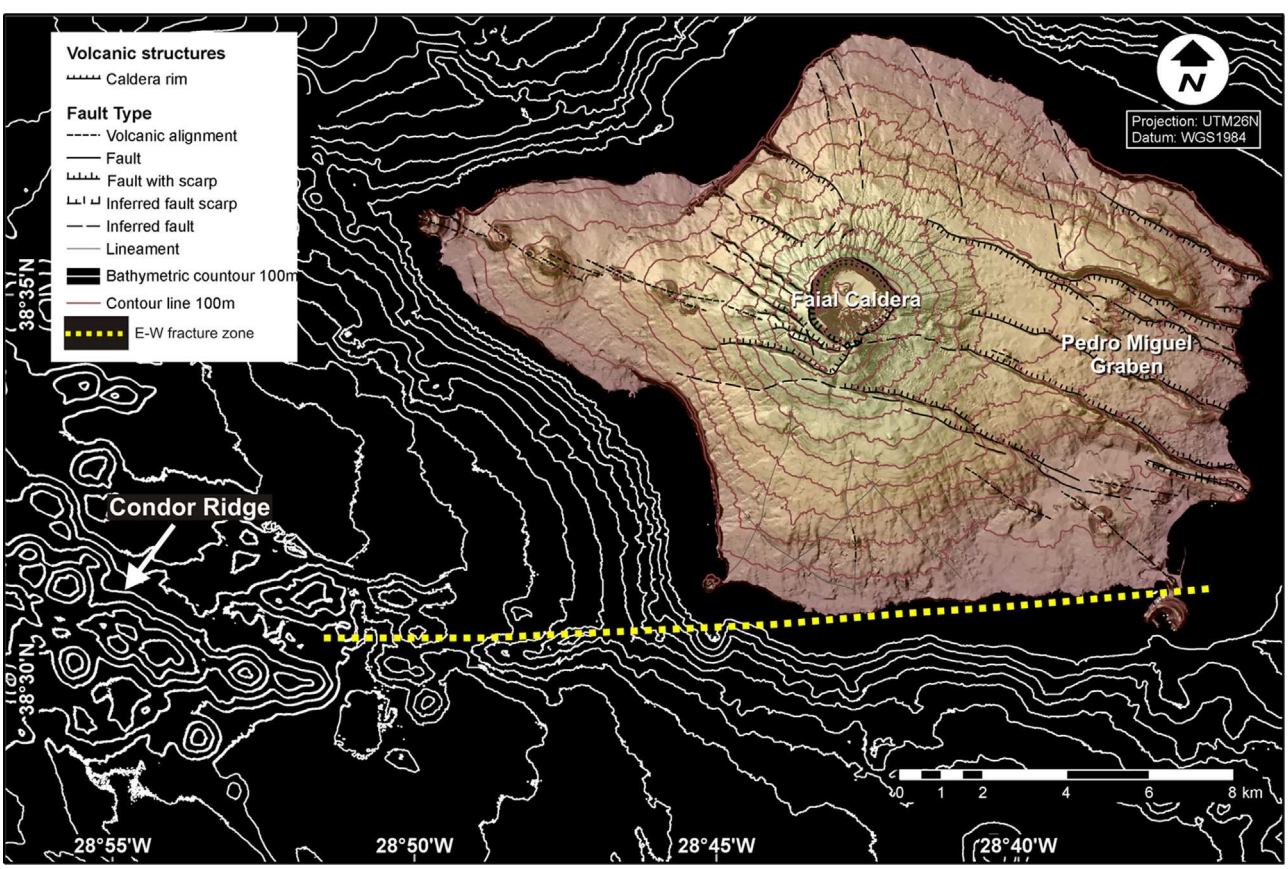

Fig. 10. Morphological expression of the E–W trending fracture zone, east of Condor seamount, to which the WNW–ESE tectonic system links. Tectonics of Faial Island from Madeira et al. (2013).

axis. Point-sources eruptive centres are particularly concentrated along lines of isolated cones, maybe due to the progressive blocking of magma ascent (*e.g.*, Head et al., 1996).

The correlation between depth and edifice type observed on the eastern end of Condor, where we have a better bathymetry resolution, can be interpreted as a result of (i) variation of hydrostatic pressure produced by the overlying water column and (ii) difficulty of magma to ascend through thicker crust and/or a less developed dyke network. Elongated edifices dominate at depths where (i) higher hydrostatic pressures reduce gas exsolution from magma favouring effusive eruptions (*e.g.* Chadwick et al., 2005; Fisher, 1984) and (ii) lower crustal thickness allow higher magma effusion rates feeding extensive fissure extrusions. In contrast, monogenetic conical edifices, predominantly formed by pyroclastic accumulations, form at shallower depths atop the few pathways persisting for magma ascending through a crust thickened by previous eruptions that built up the ridge and through a less branched dyke system farther from the rifted centre. Both cone-shaped and linear eruptive centres show preserved morphologies denoting their youth and suggest a relatively narrow age interval. The absence of dome-shaped structures and forms indicating strong explosivity (*e.g.*, large explosion or collapse pits) on both the conical and linear edifices further suggests a likely alkaline magmatic composition (basaltic *sensu latu*), as seen in their subaerial counterparts.

Distinguishing eruption style is not possible based solely on the 20 m resolution bathymetry grid used for the current analysis. At such resolution, rugged surfaces such as those forming the slopes of cones and ridges built by stacked pillow lavas may appear as smooth surfaces similar to those produced by *pahoehoe* lava flows and pyroclastic deposits.

The progressive growth of the volcanic ridge lead to decreasing hydrostatic pressures that probably contributed to a change of eruptive style. At some point, lower hydrostatic pressures, enabling higher gas exsolution (*e.g.* Moore and Schilling, 1973), may have contributed to an increased production of pyroclasts (*e.g.* Macdonald et al., 1983). The dominant smooth morphology observed on the upper central part of the ridge is interpreted as the result of deposition of large volumes of pyroclastic material.

Regarding the cones identified on the tips of the ridge, the lack of imagery, physical samples and/or seismic reflection profiles precludes a definite interpretation of their eruptive style. Although an effusive origin for these cones cannot be entirely ruled out, the (i) smooth bathymetric texture, (ii) generally consistent flank gradients and (iii) circular plan shape suggest that these cones formed by accumulation of volcaniclastic particles explosively supplied from vents located at their summits (see also Mitchell et al., 2012).

In the Azores, processes of amagmatic tectonic extension commonly become prevalent after the decline of volcanic activity, culminating in graben or hemi-graben structures (*e.g.* Jaroslow et al., 2000; Parson et al., 1993; Searle et al., 1998). This fact is testified by several islands of the archipelago, where well-developed graben structures dominate the morphology of the older inactive volcanic areas (*e.g.* Pedro Miguel graben in Ribeirinha volcano in Faial Island (Fig. 10), Serra do Cume volcano in Terceira Island, *etc.*). Unlike the well-developed tectonic pattern recognized on the seafloor around Condor, the seamount ridge still lacks purely tectonic morphologies. Similarly, gravitic failures affecting unstable sectors of the seamount flanks and resulting in mass-wasting features are limited both in size and number, despite the moderately high seismic activity of the Azores region. These incipient traces of seamount dismantling, together with the unsedimented aspect of the seamount extremities, suggest that Condor is still in a relatively early stage of its tectono-magmatic evolution.

Magnetic field data presented by Lourenço et al. (2008) show that both Condor and the ridge developing off western Faial are normally magnetized, in contrast with the negative magnetization that prevails in the surrounding sediment covered areas. They suggested that Condor formed during the Brunhes epoch, placing its formation within the last 780 Ka.

Although its emplacement in an earlier normal polarity period cannot be completely ruled out, the acoustic backscatter of the hummocky lava terrain (lacking sediment pockets and blanking) suggests a fresh and continued eruptive activity. If the seamount started to develop much earlier, a more complex pattern of both positive and negative magnetizations might also be expected.

The position of Condor in the chronology of Faial and Pico evolution remains uncertain, however, because the relationship of the eastern-most cones of Condor with the southwestern submarine slope of the Cedros Volcanic Complex (CVC; subaerial age 130–116 Ka; Hildenbrand et al., 2012) is not obvious. The subaerial development of Faial and Pico occurred approximately in the last 850 Ka (Chovelon, 1982; Féraud et al., 1980; Hildenbrand et al., 2012), a period that corresponds to the magnetic constraints.

Finally it is worth highlighting that no traces of volcanic rejuvenation were found at the eroded summit indicating volcanic quiescence on this sector of the seamount since the truncation episodes.

4.3. Erosional features

Gravitic failure is a common erosional process on volcanic seamounts (*e.g.* Mitchell, 2003; Mitchell and Lofi, 2008). Condor flanks appear to be in an early stage of erosion, exhibiting only a few slope failures and shallow relief channels.

As the seamount grew taller, gravitational stresses and flank instability were likely promoted by the growing weight of the edifice and triggered by external factors like local and regional seismicity. Higher storm wave loads impinging on a shallower summit during regression and low stands may have acted as additional forcing conditions for these events, promoting gully formation and growth along the margins of the planated seamount summit (*e.g.*, Puig et al., 2004).

4.3.1. Seamount summit truncation

Planar surfaces are common on the top of volcanic seamounts. Processes creating such morphostructures have been described by works such as those of Simkin (1972), Clague et al. (2000) or Mitchell (2001).

Condor is interpreted as a guyot that acquired its summit shape through abrasion by wave and surf action given the round boulders detected on its summit (Fig. 3A; Tempera et al., 2012).

If we consider the age constraints established by Lourenço et al. (2008), who suggest the seamount has probably formed during the Brunhes magnetic period (<780 Ka) given the polarity of the area, all planated surfaces recognized on the seamount summit (average depths: 203 m, 237 m and 303 m) are located substantially deeper than any lowstand that occurred throughout this length of time. According to Bintanja et al. (2005) glacio-eustatic sea-level fluctuations never reached below 138 m below present sea level (estimate+error) throughout the Middle and Late Pleistocene.

The three planated sectors are the result of the interplay between sea-level, elevation reached by the seamount in each moment of its evolution, thermal subsidence and loading effects by the neighbouring Faial and Pico islands. Given the scarce knowledge on (i) Condor's volcano-tectonic activity, (ii) the thermal subsidence rate affecting the underlying seafloor and (iii) the possible structural interaction with the neighbouring islands of Faial and Pico, there is an obvious complexity in reconstructing the

vertical movements of the area and no chronology can be established for the terracing events.

Despite a negative isostatic movement (subsidence) of at least 60 m has been previously suggested to explain the current bathymetric placement of the truncated surface (Tempera et al., 2012), a revised factoring of eustatic, erosional and isostatic processes suggests that it is not impossible that the summit may still have been eroded during the Last Glacial Maximum (LGM). A cumulative depth variation of the erosion horizon amounting to ~215 m below present sea level (bpsl) is obtained if we consider that

- the eustatic sea level during the LGM dropped to 135 m bpsl estimate (Yokoyama et al., 2000);
- wave erosion depth of volcaniclastic materials may have reached ~50 m depth, judging from the depth down to which historical fully wave-exposed surtseyan volcanos have been eroded following eruption. For instance, the Surtla volcano (near Surtsey, Iceland) was eroded down to 45 m depth over the 18 years following its eruption (Kokelaar and Durant, 1983) whilst volcaniclastic sediments on top of the Azorean Dom João de Castro Bank (erupted in 1720, Weston, 1964) have been terraced down to a depth of 48–56 m (Fig. 17.17 in Pascoal et al., 2006).

The vertical displacement regime affecting the seamount throughout the Holocene is unknown. Argus and Peltier (2010) model predicts a glacio-isostatic ocean floor subsidence rate of ~1–1.5 mm/yr for the area, yielding a subsidence estimate of 20–30 m, if the estimated rate is applied over the past 20 kyr. This contrasts with a present-day GPS-based analysis which indicates near-stability on the neighbouring Faial coast (see FVUL and FVAR stations on the southern shore of the Capelo peninsula in Catalão et al., 2011). It becomes plausible that some surfaces at the seamount summit may have been subject to wave erosion as late as the LGM.

4.3.2. Ploughmarks

Despite not being the best examples detected in the Azores (Tempera, unpublished multibeam data show well-defined ploughmarks on other Azores seamount tops and upper island slopes), a set of drag and bump marks identified on Condor's upper sector are identified as iceberg ploughmarks. Their dimensions and morphology are comparable to the features surveyed by multibeam sonar in Hill et al. (2008) or Dowdeswell et al. (2010). Similarly, they exhibit some bermed edges like those produced by a solid mass ploughing through seafloor sediments as well as cross-cutting relationships. Furthermore they exhibit an elongated morphology where collision occurred along flank or over a subhorizontal ground. Contrastingly, they exhibit the shape of a bump mark where collision occurred approximately perpendicular to a significant slope. The smoother aspect of the southern flank and lack of definite ploughmarks may indicate that icebergs were transported predominantly by currents from the north or that the flanks to the lee of the summit are subject to a sedimentation that has covered existing ploughmarks.

The historically very scarce use of bottom-tending trawling in the Azores region and the size of the features themselves, namely their deep indentation into the sediment, eliminate the possibility of them being the result of fishing activities in the area, virtually limited to longline and hand line. In fact only some well-located scientific trawls have been historically performed in the Azores: (i) during the Prince Albert of Monaco expeditions in the late 19th/early 20th centuries and (ii) in the course of a well-documented trawl fishery survey executed in the late 1990s. None of them ever approached the Condor area.

These ploughmarks represent an extraordinary discovery and the first record of such features in the Azores archipelago. Despite being located at an exceptionally low latitude (38°32′N), their location is still higher than of those reported by Hill et al. (2008) along the upper reaches of the Florida-Hatteras slope at 32°42′N. Given the difficulty for icebergs to arrive to the Azores in modern times, it is hypothesized that they have been emplaced during a previous glacial stage. The massive iceberg fluxes produced by glacial outburst flood events (Heinrich events) may represent the most likely recent times for icebergs to drift long distances from production zones on the North Atlantic continental margins (*e.g.*, Goff and Austin Jr., 2009). The greater storminess accompanying Heinrich events suggested by Rashid and Boyle (2007) may have contributed to their transport into the wider Atlantic areas before they melted.

5. Conclusions

The new high-resolution bathymetry and backscatter data compiled for Condor Seamount were used to map its surface geomorphology in previously unavailable detail, including a series of tectonic, volcanic and erosion features.

The seamount is shown to be a linear volcanic edifice whose shape is likely associated with the transtensional regime that prevails on the Azorean segment of the Eurasia–Nubia plate boundary, which guides the pattern of dyke intrusion. A tectonic analysis based on mapping of tectonic-related features (*e.g.*, fault scarps, volcanic cone alignments, linear eruptive centres and ridge orientation) shows that structures trending WNW–ESE to E–W dominate the area and control most of the fissural volcanism responsible for the build-up of Condor. A network of well-developed faults trending NNW–SSE was identified on areas of older ocean floor located to the N, NW and SE of Condor, which show little relation with the distribution and shape of volcanic edifices or with post-volcanic dismantling of the edifice, despite their probably presence beneath the complex.

Based on our substrate interpretation, 32% of the seamount surface consists of highly backscattering ground likely corresponding to consolidated substrates. The remaining 68% show a low uniform backscatter interpreted as unconsolidated sediment or volcaniclastic surfaces. Highly reflective ground predominates down to 800 m depth, with unconsolidated sediments dominating below that depth.

Constructional volcanic forms in the high backscatter areas include (i) linear eruptive centres, (ii) volcanic cones with and without craters, (iii) lava flows and (iv) hummocky sectors. A variation in eruptive style with depth (dominantly effusive in deeper areas *vs.* explosive in shallower areas) is suggested to explain the predominance of highly backscattering volcanic cones and hummocky terrain on the seamount extremities and the smooth sedimentary blanket that spreads out radially from the shallowest parts of the ridge.

Erosional features identified on the seamount include primarily (i) paleo wave-cut platforms on the seamount summit, (ii) landslide scars produced by lateral collapses of the NE and SW-facing flanks, (iii) gullies and turbidity current channels, and (iv) relic iceberg ploughmarks.

Taking into account its reasonably intact morphology (exhibiting a lack of well-developed tectonic deformation; a small number of erosive incisions on the flanks despite its location in an important seismogenic region; and young and unsedimented aspect of the seamount extremities), we infer that Condor must be a young seamount. On the other hand, the lack of fresh volcanic features on the eroded summit suggests that volcanic activity on the seamount summit has not occurred since the truncation episodes.

Acknowledgments

IMAR-DOP/UAz is Research and Development Unit no. 531 and LARSyS-Associated Laboratory no. 9 funded by the Portuguese Foundation for Science and Technology (FCT) through multi-annual and programmatic funding schemes (OE, FEDER, POCI2001, FSE) and by the Azores Directorate for Science and Technology (DRCT) through funding schemes (FEDER, POCI2001, FSE, COMPETE and project PEst-OE/EEI/LA0009/2011-2014). FT has been supported by a CoralFish contract (2008–2011) and an ongoing post-doctoral grant (ref. SFRH/BPD/79801/2011) from the Foundation for Science and Technology (Portugal). Surveys and data analysis were supported by projects CORALFISH (FP7 ENV/2007/1/213144), CONDOR (EEA Grants PT0040/2008), CORAZON (FCT/PTDC/MAR/72169/2006), STRIPAREA (POCI/CTE-GIN/59653/2004), HERMIONE (EC/FP7-226354) and MeshAtlantic (AA-10/1218525/BF). EMEPC is acknowledged for conducting an opportunistic multibeam survey of the seamount, sharing video imagery of ROV *Luso* dives and providing the ROV for the CORALFISH 2010 cruise. Joaquim Luís is acknowledged for sharing multibeam data from the STRIPAREA cruise. Marco Ligi (Istituto di Scienze Marine, CNR, Bologna, Italy) is acknowledged for sharing the TOBI data collected during the AZZORRE′99 cruise, which were processed by ISMAR scientists. Bathymetry sourced from GEBCO 08 Gridded Global Bathymetry is published by the British Oceanographic Data Centre on behalf of IOC and IHO. Greenpeace is acknowledged for sharing seafloor imagery from the Azores leg of the 2006 "Defending our Oceans" expedition. Ricardo Serrão Santos, Filipe Porteiro and Gui Menezes (DOP/UAz) are acknowledged for coordination and support throughout the projects mentioned above.

The authors appreciated and acknowledge the two reviewers for their thorough and helpful comments which contributed to improve this manuscript.

References

Argus, D.F., Peltier, W.R., 2010. Constraining models of postglacial rebound using space geodesy: a detailed assessment of model ICE-5G (VM2) and its relatives. Geophys. J. Int. 181, 697–723.
Bintanja, R., Van de Wal, R.S.W., Oerlemans, J., 2005. Modelled atmospheric temperatures and global sea levels over the past million years. Nature 437, 125–128.
Blondel, P., Murton, B.J., 1997. Handbook of Seafloor Sonar Imagery. John Wiley and Sons, New York p. 314.
Cannat, M., Briais, A., Deplus, C., Escartín, J., Georgen, J.L., Mercouriev, S., Meyzen, C., Muller, M., Pouliquen, G., Rabain, A., Silva, P., 1999. Mid-Atlantic Ridge – Azores hotspot interactions: along-axis migration of a hotspot-derived event of enhanced magmatism 10 to 4 Ma ago. Earth Planet. Sci. Lett. 173, 257–269.
Catalão, J., Nico, G., Hanssen, R., Catita, C., 2011. Merging GPS and atmospherically corrected InSAR data to map 3-D terrain displacement velocity. IEEE Trans. Geosci. Remote Sens. 49 (6), 2354–2360.
Carmo, R., Madeira, J., Ferreira, T., Queiroz, G. & Hipólito, A., Volcano-tectonic structures of S. Miguel Island, Azores. In: Gaspar, J.L., Guest, J.E., Duncan, A.M., Chester, D., Barriga, F. (Eds.), Volcanic Geology of S. Miguel Island (Azores Archipelago), Geol. Soc. London Mem, in press.
Chadwick Jr., W.W., Embley, R.W., Johnson, P.D., Merle, S.G., Ristau, S., Bobbitt, A., 2005. The submarine flanks of Anatahan Volcano, commonwealth of the Northern Mariana Islands. J. Volcanol. Geotherm. Res 146, 8–25.
Chovelon, P., 1982. Évolution volcanotectonique des îles de Faial et de Pico. Paris-Sud University, Centre d′Orsay p. 186. (M.Sc. thesis).
Clague, D.A., Moore, J.G., Reynolds, G.R., 2000. Formation of flat-topped volcanic cones in Hawaii. Bull. Volcanol. 62, 214–233.
DeMets, C., Gordon, R.G., Argus, D.F., Stein, S., 1994. Effect of recent revisions to the magnetic reversal time scale on estimates of current plate motions. Geophys. Res. Lett. 21, 2191–2194.
DeMets, C., Gordon, R.G., Argus, D.F., 2010. Geologically current plate motions. Geophys. J. Int. 181, 1–80.
Dias, N.A., Matias, L., Lourenço, N., Madeira, J., Carrilho, F., Gaspar, J.L., 2007. Crustal seismic velocity structure near Faial and Pico Islands (Azores), from local earthquake tomography. Tectonophysics 445, 301–317.
Dowdeswell, J.A., Jakobsson, M., Hogan, K.A., O'Regan, M., Backman, J., Evans, J., Hell, B., Löwemark, L., Marcussen, C., Noormets, R., Ó. Cofaigh, C., Sellén, E., Sölvsten, M., 2010. High-resolution geophysical observations of the Yermak Plateau and northern Svalbard margin: implications for ice-sheet grounding and deep-keeled icebergs. Quat. Sci. Rev. 29, 3518–3531.
Favalli, M., Karátson, D., Mazzarini, F., Pareshi, M.T., Boshi, E., 2009. Morphometry of scoria cones located on a volcano flank: a case study from Mt. Etna (Italy), based on high-resolution LiDAR data. J. Volcanol. Geotherm. Res. 186, 320–330.
Féraud, G., Kaneoka, I., Allegre, C.J., 1980. K/Ar ages and stress pattern in the Azores: dynamic implications. Earth Planet. Sci. Lett. 46, 275–286.
Fernandes, R.M.S., Ambrosius, B.A.C., Noomen, R., Bastos, L., Wortel, M.J.R., Spakman, W., Govers, R., 2003. The relative motion between Africa and Eurasia as derived from ITRF2000 and GPS data. Geophys. Res. Lett. 30 (16), 1,828, 5.
Fisher, R., 1984. Submarine volcaniclastic rocks. Geol. Soc. London Spec. Publ. 16 (1), 5–27.
Fornari, D.J., Batiza, R., Allan, J.F., 1987. Irregularly shaped seamounts near the East Pacific Rise: implication for seamount origin and rise axis processes. In: Keating, B.H., Fryer, P., Batiza, R., Boehlert, G.W. (Eds.), Seamounts, Islands, and Atolls. AGU (American Geophysical Union), Washington, DC, pp. 35–48.
Gaspar, J.L., 1996. Ilha Graciosa (Açores): história vulcanológica e avaliação do hazard. Azores University p. 361. (Ph.D. thesis).
Gente, P., Dyment, J., Maia, M., Goslin, J., 2003. Interaction between the Mid-Atlantic Ridge and the Azores hot spot during the last 85 Myr: emplacement and rifting of the hot spot-derived plateaus. Geochem. Geophys. Geosyst. 4 (10), 8514 (23 pp.).
Giacomello, E., Bergstad, O.A., Menezes, G., 2013. An integrated approach for studying seamounts: CONDOR observatory. Deep-Sea Res. II, this issue [10.1016/j.dsr2.2013.09.023].
Goff, J.A., Austin Jr., J.A., 2009. Seismic and bathymetric evidence for four different episodes of iceberg scouring on the New Jersey outer shelf: possible correlation to Heinrich events. Mar. Geol. 266, 244–254.
Head, J.W., Wilson, L., Smith, D.K., 1996. Mid-ocean ridge eruptive vent morphology and substructure: evidence for dike widths, eruption rates, and axial volcanic ridges. J. Geophys. Res. 101, 28265–28280.
Hildenbrand, A., Marques, F.O., Costa, A.C.G., Sibrant, A.L.R., Silva, P.F., Henry, B., Miranda, J.M., Madureira, P., 2012. Reconstructing the architectural evolution of volcanic islands from combined K/Ar, morphologic, tectonic, and magnetic data: the Faial Island example (Azores). J. Volcanol. Geotherm. Res. 241–242, 39–48.
Hill, J.C., Gayes, P.T., Driscoll, N.W., Johnstone, E.A., Sedberry, G.R., 2008. Iceberg scours along the southern U.S. Atlantic margin. Geology 36, 447–450.
Hipólito, A., Madeira, J., Carmo, R.,Gaspar, J.L. Neotectonic cs of GraciosaIsland (Azores):acontribution to seismic hazard assessment of a volcanic area in a complex geodynamic setting. Ann.Geophys, in press.
Hirn, A., Haessler, H., Hoang-Trong, P., Wittlinger, P., Mendes-Victor, L., 1980. Aftershock sequence of the January 1st, 1980 earthquake and present-day tectonics in the Azores. Geophys. Res. Lett. 7 (7), 501–504.
Höskuldsson, Á., Hey, R., Kjartansson, E., Gudmundsson, G.B., 2007. The Reykjanes Ridge between 63°10′N and Iceland. J. Geodyn. 43, 73–86.
Iyer, S.D., Mehta, C.M., Das, P., Kalangutkar, N.G., 2012. Seamounts – characteristics, formation, mineral deposits and biodiversity. Geol. Acta 10 (4), 1–14.
Jaroslow, G.E., Smith, D.K., Tucholke, B.E., 2000. Record of seamount production and off-axis evolution in the western North Atlantic Ocean, 25°25′–27°10′N. J. Geophys. Res. 105 (B2), 2721–2736.
Johnson, K.T.M., Graham, D.W., Rubin, K.H., Nicolaysen, K., Scheirer, D.S., Forsyth, D. W., Baker, E.T., Douglas-Priebe, L.M., 2008. Boomerang Seamount: the active expression of the Amsterdam-St. Paul hotspot, Southeast Indian Ridge. Earth Planet. Sci. Lett. 183, 245–259.
Kokelaar, B.P., Durant, G.P., 1983. The submarine eruption and erosion of Surtla (Surtsey), Iceland. J. Volcanol. Geotherm. Res. 19, 239–246.
Ligi, M., Mitchell, N.C., Marani, M., Gamberi, F., Penitenti, D., Carrara, G., Rovere, M., Portaro, R., Centorami, G., Bortoluzzi, G., Jacobs, C., Rouse, I., Flewellen, C., Whittle, S., Terrinha, P., Luís, J., Lourenco, N., 1999. Giant volcanic ridges amongst the Azores islands. EOS Trans. AGU, 80; p. F913. (Fall Meet. Suppl.).
Lourenço, N., Miranda, J.M., Luís, J.F., Ribeiro, A., Mendes Victor, L.A., Madeira, J., Needham, H.D., 1998. Morpho-tectonic analysis of the Azores Volcanic Plateau from a new bathymetric compilation of the area. Mar. Geophys. Res. 20 (3), 141–156.
Lourenço, N., Miranda, M., Luis, J., 2008. Principais estruturas vulcano-tectónicas submarinas em torno do Faial: uma interpretação de Mosaicos de Sonar TOBI. In: Sousa Oliveira C., Costa, A., Nunes, J.C. (Eds.). Sismo 1998 — Açores (uma década depois), pp. 221–231.
Luís, J.F., Miranda, J.M., 2008. Reevaluation of magnetic chrons in the North Atlantic between 35°N and 47°N: implications for the formation of the Azores Triple Junction and associated plateau. J. Geophys. Res. 113, B10105.
Luís, J., Miranda, J.M., Galdeano, A., Patriat, P., Rossignol, J.C., Mendes Victor, L.A., 1994. The Azores Triple Junction evolution since 10 Ma from an aeromagnetic survey of the Mid-Atlantic Ridge. Earth Planet. Sci. Lett. 125, 439–459.
Luís, J.F., Miranda, J.M., Galdeano, A., Patriat, P., 1998. Constraints on the structure of the Azores spreading center from gravity data. Mar. Geophys. Res. 20, 157–170.
Luís, J., Lourenço, N., Mata, J., Madureira, P., Miranda, J.M., Goslin, J., Perrot, J., Brachet, C., Simão, N., 2007. A highly detailed multibeam bathymetry survey of Azores Triple Junction area. Geophys. Res. Abstr. 9, 08269.
Macdonald, G.A., Abbot, A.T., Peterson, F.L., 1983. Volcanoes in the Sea the Geology of Hawaii. University of Hawai'i Press, Honolulu p. 517.
Machado, F., 1959. Submarine pits of the Azores Plateau. Bull. Volc. Ser. II XXI, 109–116.

Madeira, J., 1998. Estudos de neotectónica nas ilhas do Faial, Pico e S. Jorge: uma contribuição para o conhecimento geodinâmico da junção tripla dos Açores. Lisbon University, p. 428. (Ph.D. thesis).
Madeira, J., Brum da Silveira, A., 2003. Active tectonics and first paleoseismological results in Faial, Pico and S. Jorge islands (Azores, Portugal). Ann. Geophys. 46, 733–761.
Madeira, J., Brum da Silveira, A., Hipólito, A., Carmo, R., Active tectonics in the central and eastern Azores Islands along the Eurasia–Nubia boundary: a review. In: Gaspar, J.L., Guest, J.E., Duncan, A.M., Chester, D., Barriga, F. (Eds.). Volcanic Geology of S. Miguel Island (Azores Archipelago), Geological Society of London Memoir, in press.
Madeira, J., Ribeiro, A., 1990. Geodynamic models for the Azores triple junction: a contribution from tectonics. Tectonophysics 184, 405–415.
Madureira, P., Moreira, M., Mata, J., Allégre, J.C., 2005. Primitive helium and neon isotopes in Terceira island (Azores archipelago). Earth Planet. Sci. Lett. 233, 429–440.
McPhie, J., 1995. A Pliocene shoaling basaltic seamount: Ba volcanic group at Rakiraki, Fiji. J. Volcanol. Geotherm. Res., 64; , pp. 193–210.
Mendes, V.B., Madeira, J., Brum da Silveira, A., Trota, A., Elósegui, P., Pagarete, J., 2013. Present-day deformation in São Jorge Island, Azores, from episodic GPS measurements (2001–2011). Adv. Space Res. 51, 1581–1592.
Mitchell, N.C., 2001. The transition from circular to stellate forms of submarine volcanoes. J. Geophys. Res. 106, 1987–2003.
Mitchell, N.C., 2003. Susceptibility of mid-ocean ridge volcanic islands and seamounts to large-scale landsliding. J. Geophys. Res. 108 (B8), 2397.
Mitchell, N.C., Lofi, J., 2008. Submarine and subaerial erosion of volcanic landscapes: comparing Pacific Ocean seamounts with Valencia Seamount, exposed during the Messinian Salinity Crisis. Basin Res. 20 (4), 489–502.
Mitchell, N.C., Stretch, R., Oppenheimer, C., Kay, D., Beier, C., 2012. Cone morphologies associated with shallow marine eruptions: east Pico Island. Azores. Bull. Volcano, http://dx.doi.org/10.1007/s00445-012-0662-5.
Mitchell, N.C., Tivey, M.A., Gente, P., 2000. Seafloor slopes at mid-ocean ridges from submersile observations and implications for interpreting geology from seafloor topography. Earth Planet. Sci. Lett. 183, 543–555.
Moore, J., Schilling, J., 1973. Vesicles, water, and sulfur in Reykjanes Ridge basalts. Contrib. Mineral. Petrol. 41 (2), 105–118.
Needham, H., Francheteau, J., 1974. Some characteristics of the rift valley in the Atlantic Ocean near 36°48′ north. Earth Planet. Sci. Lett. 22, 29–43.
Ortner, H., Reiter, F., Acs, P., 2002. Easy handling of tectonic data: the programs TectonicsVB for Mac and TectonicsFP for Windows. Comput. Geosci. 28, 1193–1200.
Parson, L.M., Murton, B.J., Searle, R.C., Booth, D., Evans, J., Field, P., Keeton, J., Laughton, A., McAllister, E., Millard, N., Redbourne, L., Rouse, I., Shor, A., Smith, D., Spencer, S., Summerhayes, C., Walker, C., 1993. En echelon volcanic ridges at Reykjanes Ridge: a life cycle of volcanism and tectonics. Earth Planet. Sci. Lett. 117, 73–87.
Pascoal, A., Silvestre, C., Oliveira, P., 2006. Vehicle and mission control of single and multiple autonomous marine robots. In: Roberts, G.N., Sutton, R. (Eds.), Advances in Unmanned Marine Vehicles. IET, London, pp. 353–380.
Passaro, S., Milano, G., D'Isanto, C., Ruggieri, S., Tonielli, R., Bruno, P., Sprovieri, M., Marsella, E., 2010. DTM-based morphometry of the Palinuro seamount (Italy, Eastern Tyrrhenian Sea): geomorphological and volcanological implication. Geomorphology 115, 129–140.
Pierce, C., Sinha, M.C., 2008. Life and death of axial volcanic ridges: segmentation and crustal accretion at the Reykjanes Ridge. Earth Planet. Sci. Lett. 274 (1–2), 112–120.
Puig, P., Ogston, A.S., Mullenbach, B.L., Nittrouer, C.A., Parsons, J.D., Sternberg, R.W., 2004. Storm-induced sediment gravity flows at the head of the Eel submarine canyon, northern California margin. J. Geophys. Res. 109, C03019.
Rashid, H., Boyle, E.A., 2007. Mixed-layer deepening during Heinrich events: a multi-planktonic foraminiferal $\delta^{18}O$ approach. Science 318, 439–441.
Schilling, J.-G., 1975. Azores mantle blob: rare-earth evidence. Earth Planet. Sci. Lett. 25, 103–115.
Searle, R., 1980. Tectonic pattern of the Azores spreading centre and triple junction. Earth Planet. Sci. Lett. 51, 415–434.
Searle, R.C., Keeton, J.A., Owens, R.B., White, R.S., Mecklenburgh, R., Parsons, B., Lee, S.M., 1998. The Reykjanes Ridge: structure and tectonics of a hot-spot influenced, slow-spreading ridge, from multibeam bathymetry, gravity and magnetic investigations. Earth Planet. Sci. Lett. 160, 463–478.
Searle, R., Murton, B., Achenbach, K., LeBas, T., Tivey, M., Yeo, I., Cormier, M., Carlut, J., Ferreira, P., Mallows, C., Morris, K., Schroth, N., van Calsteren, P., Waters, C., 2010. Structure and development of an Axial Volcanic Ridge: Mid-Atlantic Ridge, 45°N. Earth Planet. Sci. Lett. 299, 228–241.
Silveira, G., Stutzmann, E., Davaille, A., Montagner, J.-P., Mendes-Victor, L., Sebai, A., 2006. Azores hotspot signature in the upper mantle. J. Volc. Geotherm. Res. 156, 23–34.
Simkin, T., 1972. Origin of some flat-topped volcanoes and guyots. Mem. Geol. Soc. Am. 132, 183–193.
Smith, D.K., Cann, J.R., 1992. The role of seamount volcanism in crustal construction along the Mid-Atlantic Ridge at 24°−30°N. J. Geophys. Res. 97, 1,645–1,658.
Smoot, N.C., 1995. Mass wasting and subaerial weathering in guyot formation: the Hawaian and Canary Ridges as examples. Geomorphology 14, 29–41.
Tempera, F., Giacomello, E., Mitchell, N.C., Campos, A.S., Braga Henriques, A., Bashmachnikov, I., Martins, A., Mendonça, A., Morato, T., Colaço, A., Porteiro, F.M., Catarino, D., Gonçalves, J., Pinho, M.R., Isidro, E.J., Santos, R.S., Menezes, G., 2012. Mapping the Condor seamount seafloor environment and associated biological assemblages (Azores, NE Atlantic). In: Harris, P.T., Baker, E.K. (Eds.), Seafloor Geomorphology as Benthic Habitat: Geohab Atlas of Seafloor Geomorphic Features and Benthic Habitats. Elsevier, London, pp. 807–818.
Vogt, P.R., Jung, W.Y., 2004. The Terceira Rift as hyperslow, hotspot dominated oblique spreading axis: a comparison with other slow spreading plate boundaries. Earth Planet. Sci. Lett. 218, 77–90.
Wessel, P., 2007. Seamount characteristics. In: Pitcher, T.J., Morato, T., Hart, P.J.B., Clark, M.R., Haggan, N., Santos, R.S. (Eds.), Seamounts: Ecology, Fisheries and Conservation. Blackwell, Oxford, UK, pp. 3–25.
Weston, F.S., 1964. List of recorded volcanic eruptions in the Azores with brief reports. Bol. Mus. Lab. Miner. Geol. Univ. Lisboa 10, 3–18.
Yesson, C., Clark, M.R., Taylor, M.L., Rogers, A.D., 2011. The global distribution of seamounts based on 30″ bathymetry data. Deep-Sea Res. I 58, 442–453.
Yokoyama, Y., Lambeck, K., De Deckker, P., Johnston, P., Fifield, L.K., 2000. Timing of the Last Glacial Maximum from observed sea-level minima. Nature 406, 713–716.
Zeppilli, D., Bongiorni, L., Cattaneo, A., Danovaro, R., Santos, R.S., 2013. Meiofauna assemblages of the Condor Seamount (North-East Atlantic Ocean) and adjacent deep-sea sediments. Deep-Sea Res. II, this issue [10.1016/j.dsr2.2013.08.009].